Engineering Applications

https://publish.mersin.edu.tr/index.php/enap

e-ISSN 2979-9201

Methods and software for estimation of total electron content in ionosphere using GNSS observations

Alexander Naumov [*1], Petr Khmarskiy [1], Nikita Byshnev [1], Mikita Piatrouski [1]

[1]Institute of Applied Physics of the National Academy of Sciences of Belarus, Belarus, naumov@iaph.bas-net.by; pierre2009@mail.ru; nick.byshnev@gmail.com; petrovskij.nico@gmail.com

Cite this study: Naumov, A., Khmarskiy, P., Byshnev, N., & Piatrouski, M. (2023). Methods and software for estimation of total electron content in ionosphere using GNSS observations. Engineering Applications, 2 (3), 243-253

Keywords
Ionosphere
Radio tomography
Total electron content
GNSS

Research Article
Received:02.08.2023
Revised: 11.10.2023
Accepted: 19.10.2023
Published:23.10.2023

Abstract

Methods and algorithms for determining the total electron content in the ionosphere by signals of global navigation satellite systems are investigated. An algorithm for calculating and visualizing vertical total electron content over the territory of the Republic of Belarus and neighboring states is developed, taking into account correction of phase ambiguity due to «cycle slip» and estimation of differential code biases. Software for processing radio-tomographic data for high-orbit ionosphere control is created. It includes tools for calculating the total electron content from the signals of the GPS satellites, tools for eliminating cycle slip, tools for calculating differential code biases, tools for calculating vertical total electron content over the territory of the Republic of Belarus and neighboring states. The software is written in the Python programming language version 3.10, using third-party cross-platform free libraries. The performance of the presented methods and algorithms is demonstrated by examples.

1. Introduction

Relevance of the study of processes occurring in the ionosphere is due to the fact that the spatial and temporal inhomogeneities of the electromagnetic field in the upper atmosphere of the Earth play an important role in the functioning of modern technological systems [1-3]. For example, maintenance of serviceability of equipment installed onboard satellites, accuracy of objects location with global navigation satellite systems, characteristics of radio-wave propagation, ground-based electrical generating, electrical and pipe-line systems operation depend on knowledge of upper atmosphere state at ionospheric heights.

One of the most effective ways to study spatial and temporal changes in ionosphere is radio sounding using high orbital navigation satellites [1-4]. Such a system includes a constellation of satellites and a set ground receiving stations. At successive discrete times, all ground stations simultaneously receive satellite radio signals. After their conversion, measurement results are obtained, the values of which are functionally related to the total electron content (TEC) which describes the number of electrons on the line connecting the satellite with the ground receiving station. These data are processed to obtain information about the state of the ionosphere in the observed area.

Recently, radio tomography has become one of the most effective tools for the study of the ionosphere. This method makes it possible to probe the ionosphere using satellite transmitters and ground receiving stations, covering a wide spatial and temporal range. Tomographic methods are used to reconstruct images of the electron concentration distribution field [1, 5].

A radio tomography system includes a group of satellites that move in circular or elliptical orbits and a network of ground receiving stations. One of the important advantages of radio tomography is the ability to obtain

information on changes in the electron concentration field in the ionosphere in real time. That makes it possible to ensure the stability of the operation of technologies and communication systems that depend on the state of the ionosphere.

The development and evolution of global satellite navigation systems, such as GPS, GLONASS, Beidou, Galileo and others, had opened up new opportunities for ionospheric research. These systems provide valuable data that can be used for radio tomography and a better understanding of the state of the ionosphere. Many research centers all over the world (especially in USA, China, Poland, Japan, Malaysia, Belgium, France, Russia, Spain, Italy and other) are engaged in the study of ionospheric radio tomography [3, 6-14]. In spite of this, there are still important scientific and practical tasks in this field.

Currently, there is a network of 96 continuously operating points of the precise positioning satellite system of the Republic of Belarus (SSTP RB), which can be used for measurements. Data from these stations allow us to calculate TEC. Based on the TEC, the vertical total electron content (VTEC), which characterizes the integral concentration of electrons in a vertical column above a given point on the Earth's surface, can be found.

2. Material and Method

2.1. Total electron content calculation

The prorogation of electromagnetic signals through the ionosphere depends on the concentration of free electrons in it. In addition, the effect of the ionosphere on radio signals depends on the frequency of the signal, i.e., ionosphere is a dispersing medium. This effect changes the speed of propagation of signals with respect to the speed of light due to the presence of a refractive index other than 1. Depending on whether the group or phase of the signal is considered, these refractive indices will be different. They are related by the Equation 1 [15, 16]:

$$n_{gr} = n_{ph} + f\frac{dn_{ph}}{df} \tag{1}$$

where n_{gr} and n_{ph} are refractive indices for group and phase signals, f - signal frequency.

The total electron content is defined as the integral of the electron density along the path between the satellite and the receiving station, Equation 2 [15,16]:

$$TEC = \int_S n_e(s)ds \tag{2}$$

It is expressed in TEC Units (TECU), where 1TECU is defined as 10^{16} electrons contained in a cylinder with a cross section of 1 m^2, aligned with the beam path. TEC can be calculated by the Equation 3 and 4 [15]:

$$TEC_{gr} = \frac{1}{40{,}28}\left(\frac{f_1^2 f_2^2}{f_1^2 - f_2^2}\right)[P_2 - P_1 + c(D_r + D_s)] \tag{3}$$

$$TEC_{ph} = \frac{1}{40{,}28}\left(\frac{f_1^2 f_2^2}{f_1^2 - f_2^2}\right)\left[L_1 - L_2 - \lambda_1 N_1 + \lambda_2 N_2 + c\left(D_r + D_s\right)\right] \tag{4}$$

where λ_1 and λ_2 are wavelengths corresponding to frequencies f_1 and f_2, P_1 and P_2 are pseudoranges measurements in meters, L_1 and L_2 are phase measurements in meters, c is the velocity of light in the vacuum, N_1 and N_2 are phase ambiguities due to the integer number of wavelengths at the measurement distance, D_s и D_r are the differential code biases for the satellite and receiver respectively.

As an example, in the Figure 1 raw pseudoranges data from 5 GPS satellites (G01-G05) are presented. TEC calculations were performed with the so-called non-geometric linear combination of two frequencies L_1 and L_2, which contains only ionospheric information. In the Figure 2 the corresponding TEC values calculated from the pseudorange differences are shown, while in the Figure 3 the TEC values calculated from the phase differences are presented. It can be seen that the TEC values obtained from the phase data are less noisy, but contain an additive error.

2.2. Correction of cycle slip and estimation of differential code biases

TEC derived from phase measurements are less noisy than those derived from code measurements, it is additionally necessary to correct phase ambiguity and errors associated with cycle slip in receiving equipment [4].

For this purpose, the method described in [17] was used. It is based on the calculation of the mean value and standard deviation of the double-differenced ionospheric-free observations in each of the observation epochs. The epoch is defined as the time of continuous observation of the signal when the data is not interrupted by more than a given amount (for example, 60 seconds). In the case when the observed value differs from the average value in the previous epoch by more than 6 standard deviations, the cycle slip is considered detected and an appropriate correction is introduced to eliminate the cycle slip.

In this work, we used a method based on [18-20] to estimate the differential code biases D_s (satellite) and D_r (receiver). In this method a set of linear equations is constructed that relates the observed values of TEC, the values of the vertical total electron content and unknown differential code biases. Using the least squares approach we can solve this set of equation and estimate the differential code biases.

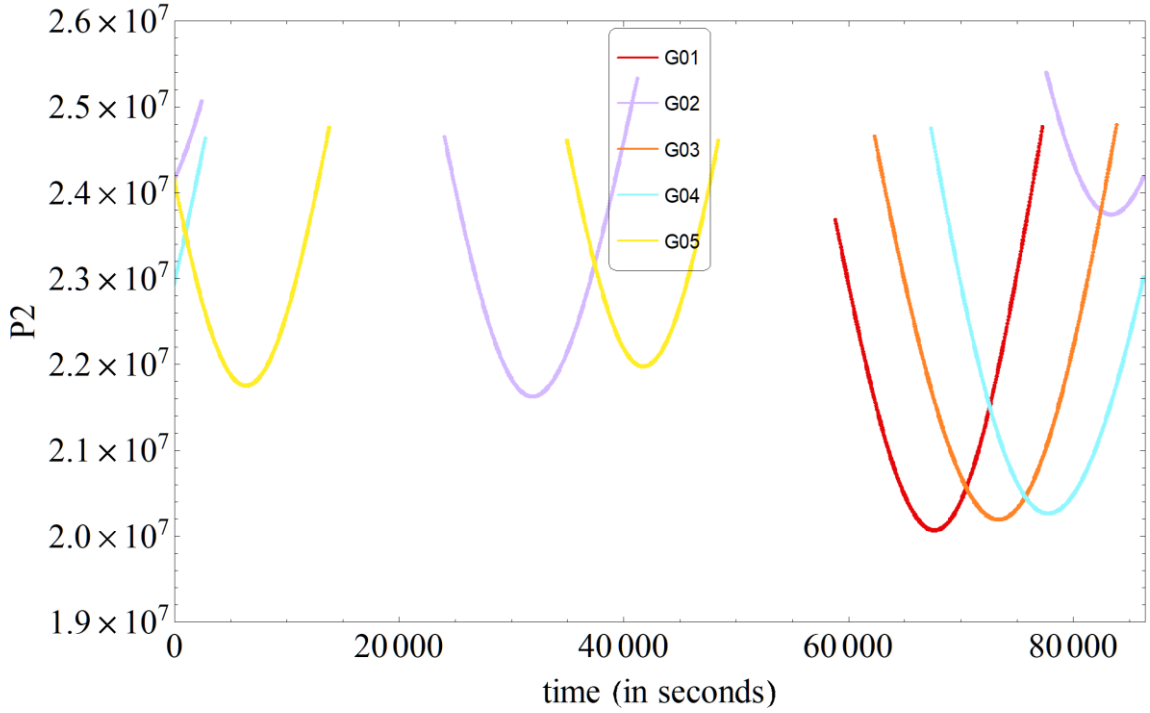

Figure 1. Example of raw pseudoranges data from GPS satellites.

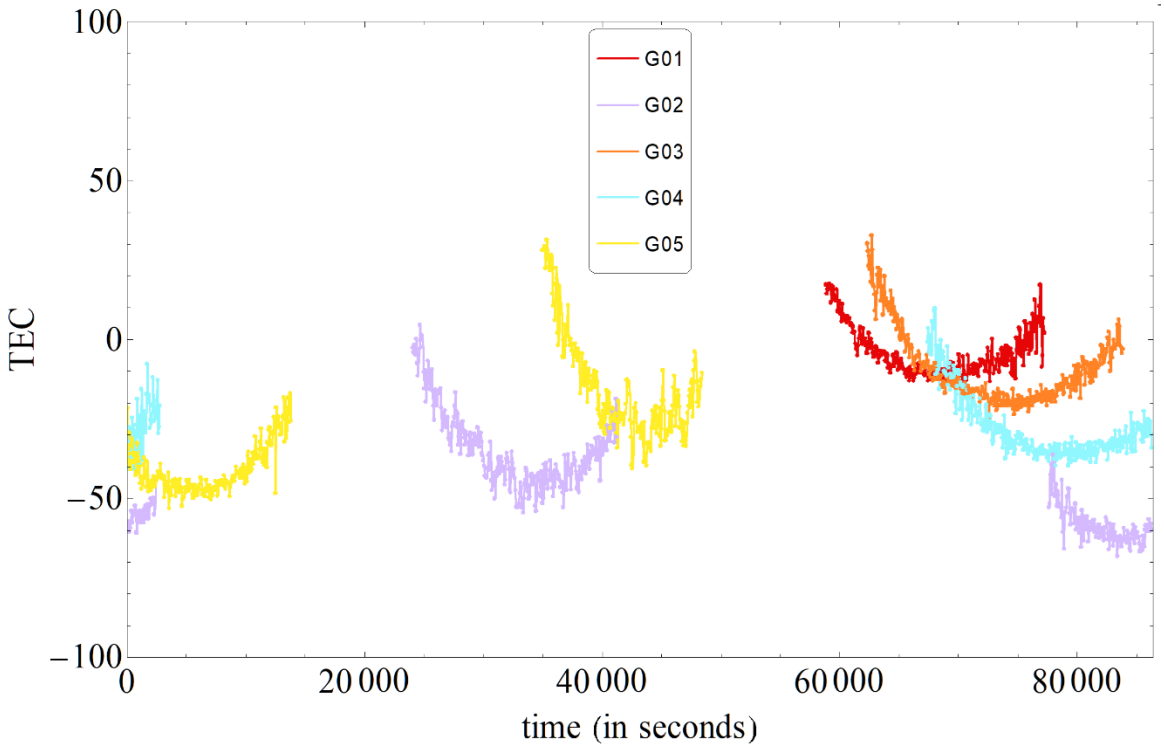

Figure 2. Example of TEC calculation using pseudorange data.

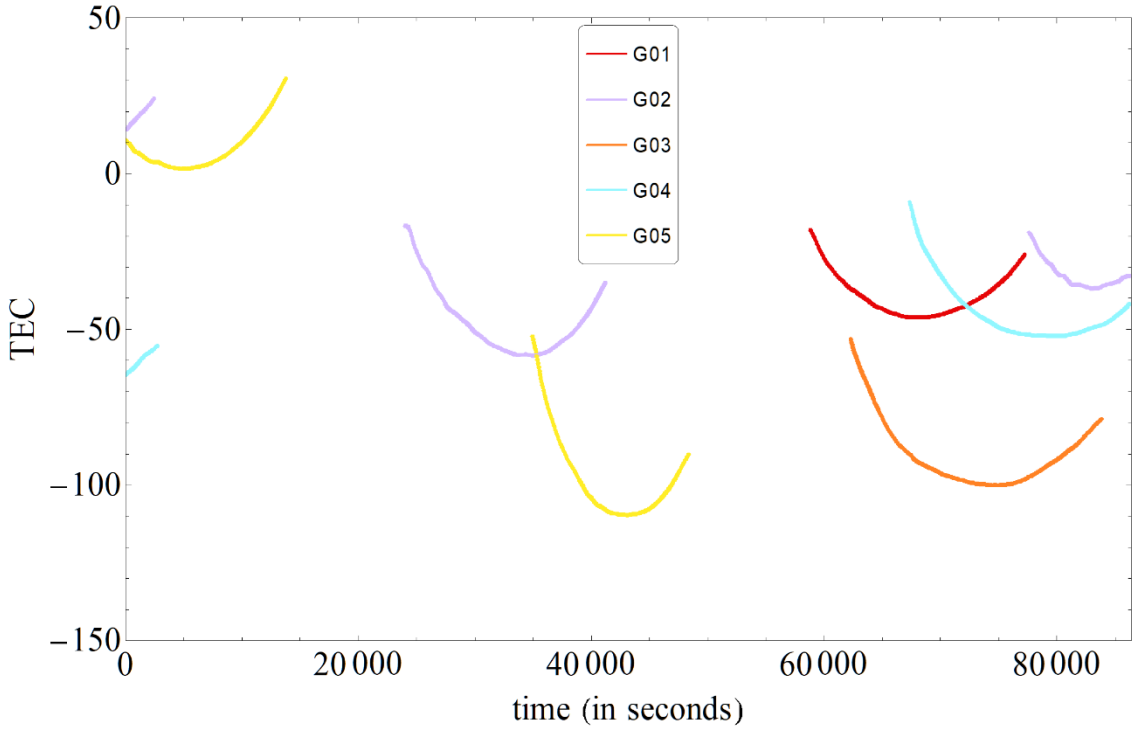

Figure 3. Example of TEC calculation using phase data.

2.3. Vertical total electron content calculation

For a number of problems, the TEC value is not very convenient, because, firstly, it strongly depends on the angle of elevation of the satellite, and, secondly, it cannot be referred to any specific point of space. More convenient is a quantity called the vertical total electron content, which is defined as the integral concentration of electrons in a vertical column above the Earth's surface. For this purpose, some height h is chosen, at which the center of gravity of the electron concentration is located. The point at this chosen height is called the Ionospheric Pierce Point (IPP) and is defined as a point on the beam connecting the satellite to the receiver at the chosen height above the Earth's surface. In the following calculations, this altitude was set to h = 504 km.

To determine the vertical total electron content, at the first stage it is necessary to calculate the satellite position parameters. Here below the algorithm used to calculate the position of a GPS satellite based on navigation data [21] are described:

1) Calculate time t_k from reference ephemeris epoch t_{oe} (t_k and t_{oe} expressed in seconds during the GPS week) (Equation 5):

$$t_k = t - t_{oe} \tag{5}$$

If $t_k > 302\,400$ c, $t_k = t_k - 604\,800$. If $t_k < -302\,400$ c, $t_k = t_k + 604\,800$.

2) Calculate the mean anomaly (Equation 6) for t_k:

$$M_k = M_0 + \left(\frac{\sqrt{\mu}}{\sqrt{a^3}} + \Delta n\right) t_k \tag{6}$$

3) Iteratively solve the Kepler equation for the eccentric anomaly E_k:

$M_k = E_k - e\sin E_k$.

4) Calculate true anomaly (Equation 7) v_k:

$$v_k = \arctan \frac{\sqrt{1-e^2}\sin E_k}{\cos E_k - e} \tag{7}$$

5) Calculate latitude argument u_k (Equation 8) from perigee argument ω, true anomaly v_k, using correction coefficients c_{uc} and c_{us}:

$$u_k = \omega + v_k + c_{uc}\cos 2(\omega + v_k) + c_{us}\sin 2(\omega + v_k) \tag{8}$$

6) Calculate radial distance r_k (Equation 9), using correction coefficients c_{rc} and c_{rs}:

$$r_k = a(1 - e\cos E_k) + c_{rc}\cos 2(\omega + v_k) + c_{rs}\cos 2(\omega + v_k) \quad (9)$$

7) Calculate the orbital inclination i_k (Equation 10) from the inclination i_o at the reference time using the correction coefficients c_{ic} and c_{is}:

$$i_k = i_0 + it_k + c_{ic}\cos 2(\omega + v_k) + c_{is}\sin 2(\omega + v_k) \quad (10)$$

8) Calculate the longitude of the ascending node λ_k (relative to Greenwich Mean Time) (Equation 11). This calculation uses right ascension at the beginning of the current week (Ω_0), a correction for the apparent variation in sidereal Greenwich Mean Time between the start of the week and the reference time $t_k = t - t_{oe}$, and the change in the longitude of the ascending node from the time reference:

$$\lambda_k = \Omega_0 + \left(\dot{\Omega} - \omega_E\right)t_k - \omega_E t_{oe} \quad (11)$$

9) Calculate ground coordinates by applying three rotations (around u_k, i_k and λ_k) (Equation 12):

$$\begin{bmatrix} X_k \\ Y_k \\ Z_k \end{bmatrix} = R_3(-\lambda_k)R_1(-i_k)R_3(-u_k)\begin{bmatrix} r_k \\ 0 \\ 0 \end{bmatrix} \quad (12)$$

where R1 and R3 are the rotation matrices, defined in [21].

Further, after determining the position of the satellite and the receiver, it is necessary to calculate the elevation angle χ in the IPP using the elevation angle of satellite α by Equation 13:

$$\chi = \arcsin\frac{R_e\cos\alpha}{R_e + h} \quad (13)$$

After that, the vertical total electron content (VTEC) is calculated from the TEC values (Equation 14):

$$VTEC = TEC \cdot \cos\chi \quad (14)$$

3. Results

Software for processing data of high-orbit ionosphere control provides implementation of methods and algorithms for obtaining, processing and storing information about ionosphere conditions over the territory of the Republic of Belarus and neighboring countries. This software uses radio signals from high-orbit navigation satellite systems, obtained by the precise positioning satellite system of the Republic of Belarus. The software will be a part of space system of radiometric control of near-Earth space based on satellite systems and specialized ground facilities, which will make it possible to increase the safety level of operation of complex infrastructure objects on the territory of the Republic of Belarus.

The software is written in the Python programming language version 3.10, using third-party cross-platform free libraries Matplotlib, NumPy, Plotly, SciPy, georinex, Pandas, pymap3d, Xarray, PyKrige, GeoPandas. The software provides the following operations:

- reading observation data from the SSTP RB in RINEX format [22];
- reading navigation data of GPS satellites in RINEX format;
- calculation of parameters of orbits of satellites of the GPS system;
- calculation of the total electron content according to the data of navigation satellites of the GPS system;
- elimination of cycle slip in the data obtained from phase measurements;
- calculation of differential code biases for SSTP RB stations and GPS satellites;
- calculation of vertical total electron content over the territory of the Republic of Belarus and neighboring states;
- displaying the results of calculation of the TEC in the form of color graphs;
- saving the results of TEC and VTEC calculation in “csv” format;
- visualization of the calculation results of the vertical total electron content.

Figure 4 shows the values of total electron content before the cycle slip correction, obtained from the phase pseudorange of GPS satellite signals for May 5, 2022, between 00:00:00 and 01:00:00 UTC. Figure 5 shows the same values after the cycle slip correction. It can be seen that the outliers associated with slippage are effectively corrected by the used algorithm.

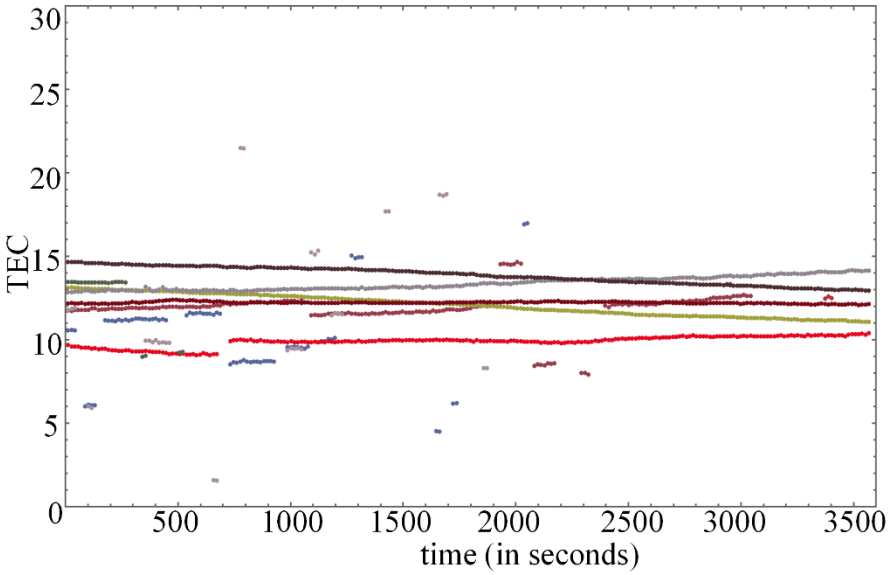

Figure 4. Values of total electron contents before cycle slip correction.

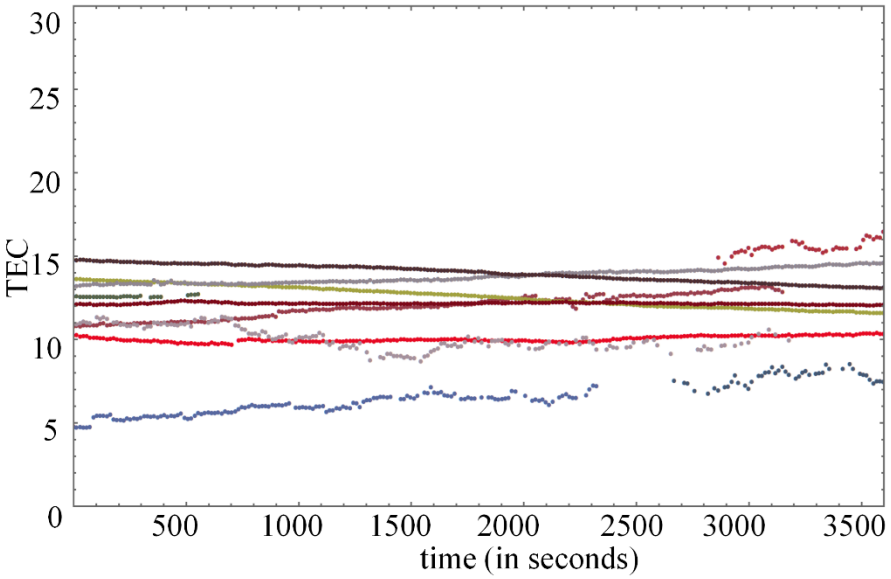

Figure 5. Values of total electron contents after cycle slip correction.

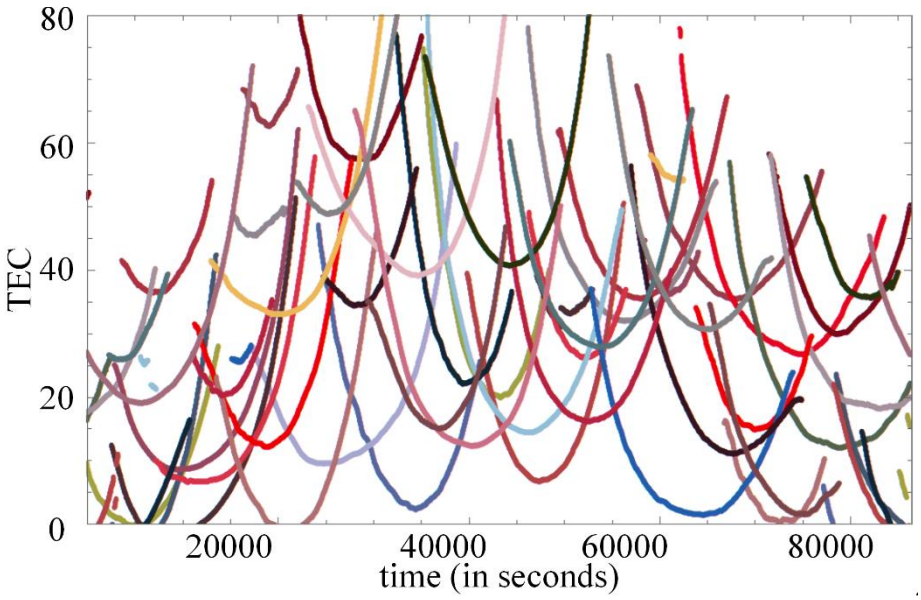

Figure 6. TEC values before correction of differential code biases.

As an example of the operation of the algorithm for determining the differential code biases, we present the results of calculation of the total electron content using data from May 5, 2022 from the observation station "bori", located in the city of Borisov. Figure 6 shows the values of total electron content before the correction of differential code biases for all 32 GPS satellites. Figure 7 shows the same values after the differential code biases correction.

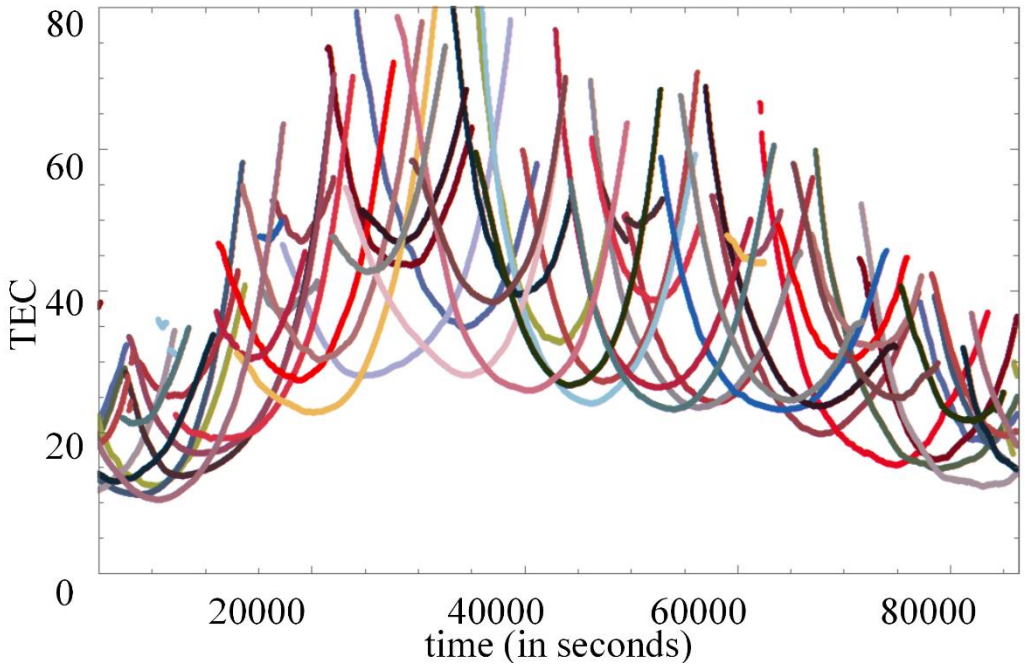

Figure 7. TEC values after correction of differential code biases.

In the Figure 8 the results of calculating the vertical total electron content for all 32 GPS satellites according to data from May 5, 2022 from the observation station "bori" located in the city of Borisov are shown. It is clearly seen that, in comparison with the values of the slant electron content in the Figure 7, the vertical total electron content values do not include outliers at the extreme observation points, which, in the case of a slant electron content, are due to the low elevation angle of the satellite.

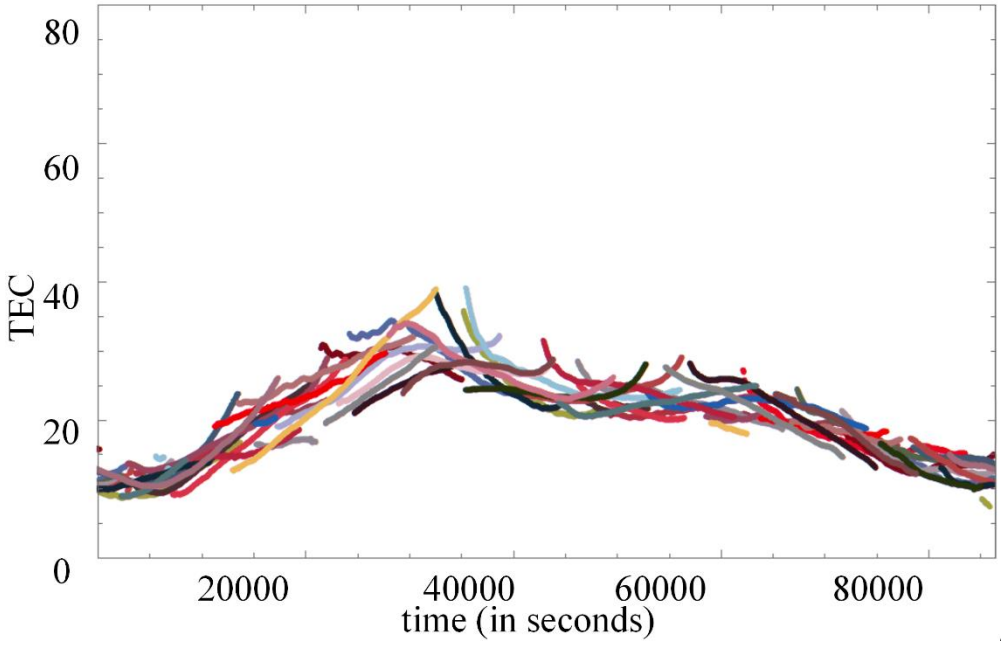

Figure 8. VTEC values calculated using GPS satellites.

Figure 9 shows the results of vertical total electron content (VTEC) calculation compared to slant total electron (STEC) values. A significant increase in VTEC values during time from 6 o'clock (sunrise) to 21 o'clock (sunset) with a peak at 14 o'clock (time when the sun is at zenith) is clearly visible.

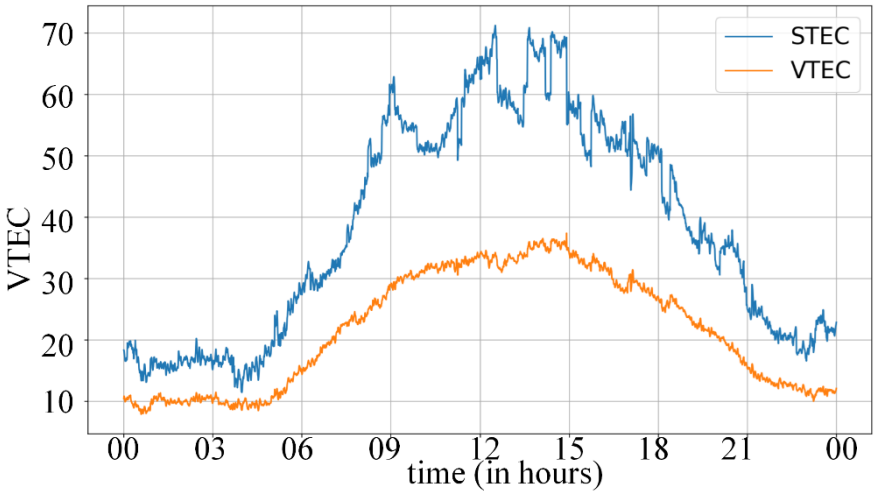

Figure 9. VTEC values averaged over all satellites by code pseudodistance and their corresponding STEC values.

Calculation of the vertical electron content over the territory of the Republic of Belarus was carried out using software tools for processing data of ionosphere high-orbit control. The output of these software tools is the calculation, interpolation and visualization of the vertical electron content for a given area. Figure 10 shows examples of calculation of vertical electron content (VTEC) over the territory of the Republic of Belarus based on data from 96 ground receiving stations at different moments of time. It can be seen that in general over the territory of the Republic of Belarus the vertical electron content is distributed uniformly without sharp jumps and significant inhomogeneities.

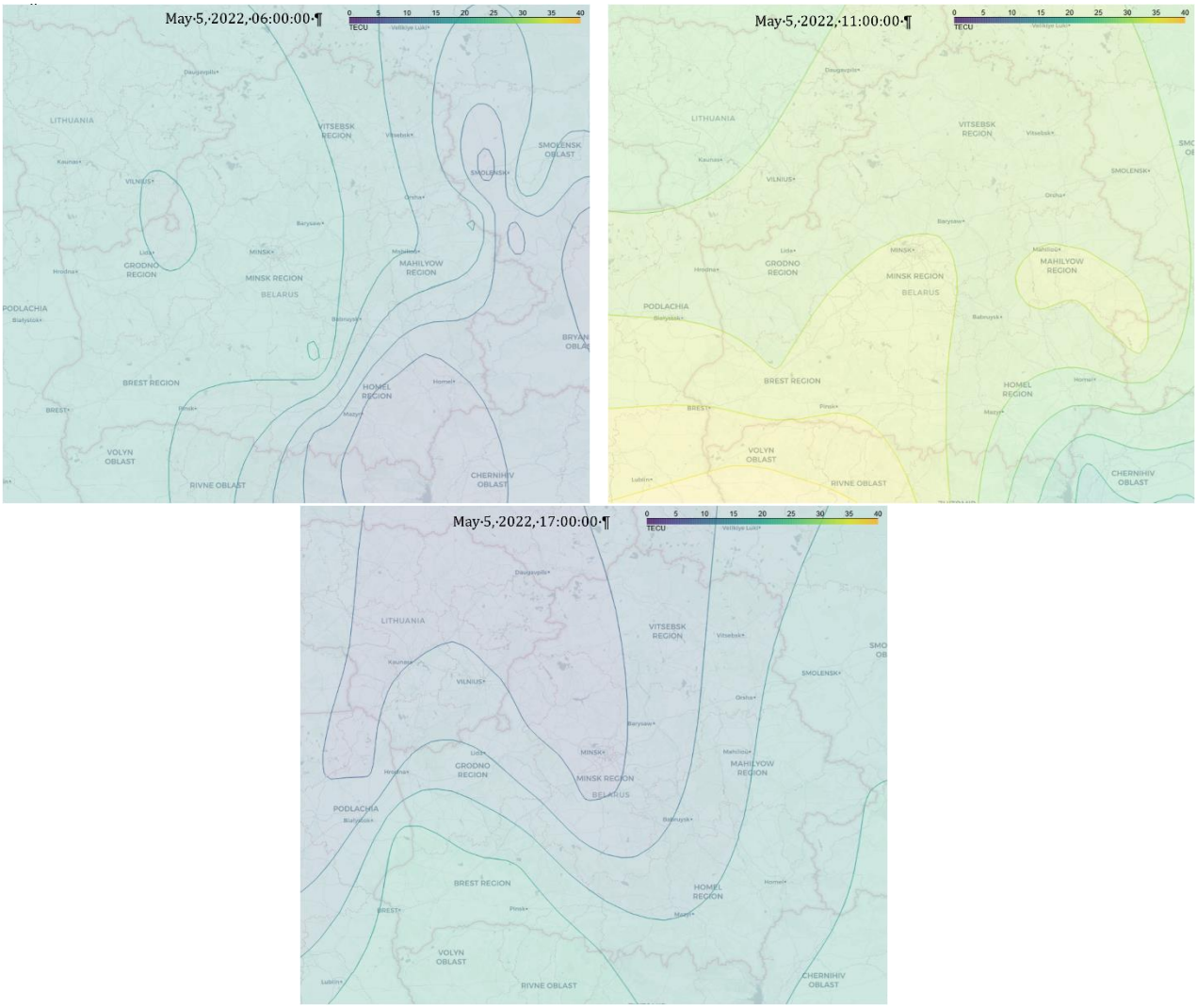

Figure 10. Example of calculation of vertical total electron content over the territory of the Republic of Belarus.

4. Discussion

The results obtained are of important practical and scientific interest. First, experimental results of the study of the ionosphere structure over the territory of the Republic of Belarus and neighboring states are demonstrated. Experimental data of the precise positioning satellite system of the Republic of Belarus were used.

Taking into account the obtained experimental information about the electron concentration in the ionosphere over the territory of the Republic of Belarus is of great importance for the development of satellite radio navigation, long-range radio communication systems, radar systems and other technologies in the republic. The assessment of this information makes it possible to forecast and understand the state of the ionosphere over the territory of the Republic of Belarus and neighboring states, which, in turn, contributes to improving the performance of communication, location and navigation systems.

In addition, the assessment of the levels of electron concentration fields in the ionosphere over the territory of the Republic of Belarus and neighboring states is important for the study of the propagation of radio waves in the atmosphere, the study of climate and the understanding of natural hazards [23,24]. Knowledge of the state of the ionosphere makes it possible to take into account its influence on the propagation of radio waves, to assess the impact of ionospheric disturbances on climatic processes and to forecast ionospheric hazards [23-25].

Thus, the estimation of electron concentration in the ionosphere has a wide range of practical applications and plays an important role in scientific research, which is aimed at the development and improvement of communication, navigation technologies and understanding of atmospheric and ionospheric processes.

5. Conclusion

Experimental studies of the total electron content in the ionosphere above the Republic of Belarus were carried out. The data were collected using global navigation satellite systems and ground receiving stations of the precision positioning system of the Republic of Belarus. As a result of the analysis of the structure of the ionosphere, expressions for calculating the total electron content using a dual-frequency measurement method combining phase and code biases of radio signals were presented. The results of the algorithm for eliminating the cycle slip and determining the differential code biases before and after correction were also demonstrated.

The Python 3.10 programming language was used to work with the data, using third-party cross-platform free libraries. The paper also provides examples of calculation of vertical electron content over the Republic of Belarus at the different moments of time. In the future it is planned to develop and study methods of three-dimensional reconstruction of electron distribution in the ionosphere on the basis of the obtained data.

Acknowledgement

This study was partly presented at the 7th Advanced Engineering Days [26].

Funding

This work has been supported by State Program of the Republic of Belarus “Science-intensive technologies and engineering” for 2021-2025, project “Develop a space system for radiometric monitoring of near-Earth space based on a small spacecraft and specialized ground facilities”.

Author contributions

Alexander Naumov: Substantiation of the research concept, Formulation of ideas, Research goals and objectives, Development of methodology and Research model. **Petr Khmarskiy:** Collection and systematization of data, Comparative analysis, Writing the text of the manuscript. **Nikita Byshnev:** Generalization and Interpretation of the results of the study, Editing the text of the manuscript, Working with graphic material. **Mikita Piatrouski:** Computer programming and Mathematical modeling.

Conflicts of interest

The authors declare no conflicts of interest.

References

1. Artemiev, V. M., Naumov, A. O., Stepanov, V. L., & Murashko, N. I. (2008). Method and results of real time modeling of ionosphere radiotomography on the basis of the Kalman filter theory. Journal of Automation and Information Sciences, 40(2), 52-62. https://doi.org/10.1615/JAutomatInfScien.v40.i2.50
2. Belokonov, I. V., Krot, A. M., Kozlov, S. V., Kapliarchuk, Y. A., Savinykh, I. E., & Shapkin, A. S. (2023). A method for estimating the total electron content in the ionosphere based on the retransmission of signals from the global navigation satellite system GPS. Informatics, 20(2), 7-27. https://doi.org/10.37661/1816-0301-2023-20-2-7-27
3. Milanowska, B., Wielgosz, P., Krypiak-Gregorczyk, A., & Jarmołowski, W. (2021). Accuracy of global ionosphere maps in relation to their time interval. Remote Sensing, 13(18), 3552. https://doi.org/10.3390/rs13183552
4. Sickle, J. V. (2015). GPS for Land Surveyors. 4th ed. CRC Press, 368. ISBN 978-14-6658-310-8
5. Themens, D. R., Jayachandran, P. T., Langley, R. B., MacDougall, J. W., & Nicolls, M. J. (2013). Determining receiver biases in GPS-derived total electron content in the auroral oval and polar cap region using ionosonde measurements. GPS solutions, 17, 357-369. https://doi.org/10.1007/s10291-012-0284-6
6. Galkin, I., Froń, A., Reinisch, B., Hernández-Pajares, M., Krankowski, A., Nava, B., ... & Batista, I. (2022). Global monitoring of ionospheric weather by GIRO and GNSS data fusion. Atmosphere, 13(3), 371. https://doi.org/10.3390/atmos13030371
7. Zakharenkova, I., Cherniak, I., Braun, J. J., & Wu, Q. (2023). Global Maps of Equatorial Plasma Bubbles Depletions Based on FORMOSAT-7/COSMIC-2 Ion Velocity Meter Plasma Density Observations. Space Weather, 21(5), e2023SW003438. https://doi.org/10.1029/2023SW003438
8. Yasyukevich, Y., Mylnikova, A., & Vesnin, A. (2020). GNSS-based non-negative absolute ionosphere total electron content, its spatial gradients, time derivatives and differential code biases: bounded-variable least-squares and taylor series. Sensors, 20(19), 5702. https://doi.org/10.3390/s20195702
9. Juan, J. M., Sanz, J., Rovira-Garcia, A., González-Casado, G., Ibáñez, D., & Perez, R. O. (2018). AATR an ionospheric activity indicator specifically based on GNSS measurements. Journal of Space Weather and Space Climate, 8, A14. https://doi.org/10.1051/swsc/2017044
10. Rideout, W., & Coster, A. (2006). Automated GPS processing for global total electron content data. GPS solutions, 10, 219-228. https://doi.org/10.1007/s10291-006-0029-5
11. Roma-Dollase, D., Hernández-Pajares, M., Krankowski, A., Kotulak, K., Ghoddousi-Fard, R., Yuan, Y., ... & Gómez-Cama, J. M. (2018). Consistency of seven different GNSS global ionospheric mapping techniques during one solar cycle. Journal of Geodesy, 92, 691-706. https://doi.org/10.1007/s00190-017-1088-9
12. Li, Z., Wang, N., Hernández-Pajares, M., Yuan, Y., Krankowski, A., Liu, A., ... & Blot, A. (2020). IGS real-time service for global ionospheric total electron content modeling. Journal of Geodesy, 94, 32. https://doi.org/10.1007/s00190-020-01360-0
13. Lean, J. L., Meier, R. R., Picone, J. M., Sassi, F., Emmert, J. T., & Richards, P. G. (2016). Ionospheric total electron content: Spatial patterns of variability. Journal of Geophysical Research: Space Physics, 121(10), 367-402. https://doi.org/10.1002/2016JA023210
14. Huang, C., Lu, G., Zhang, Y., Paxton, L. J. (2021). Ionosphere Dynamics and Applications. American Geophysical Union and Wiley. ISBN 9781119507550.
15. Hofmann-Wellenhof, B. (2008). GNSS – Global Navigation Satellite Systems. GPS, GLONASS, Galileo, and more. Springer, Berlin, Germany. ISBN 978-3-211-73017-1
16. Materassi, M., Forte, B., Coster, A., Skone, S. (2020). The Dynamical Ionosphere A Systems Approach to Ionospheric Irregularity. Elsevier. ISBN 978-0-12-814782-5.
17. Hieu, L. V., Ferreira, V. G., He, X., & Tang, X. (2014). Study on cycle-slip detection and repair methods for a single dual-frequency global positioning system (GPS) receiver. Boletim de Ciências Geodésicas, 20(4), 984-1004. https://doi.org/10.1590/S1982-21702014000400054
18. Wang, Y., Zhao, L., & Gao, Y. (2021). Estimation and analysis of GNSS differential code biases (DCBs) using a multi-spacing software receiver. Sensors, 21(2), 443. https://doi.org/10.3390/s21020443
19. Wang, N., Yuan, Y., Li, Z., Montenbruck, O., & Tan, B. (2016). Determination of differential code biases with multi-GNSS observations. Journal of Geodesy, 90, 209-228. https://doi.org/10.1007/s00190-015-0867-4
20. Montenbruck, O., Hauschild, A., & Steigenberger, P. (2014). Differential code bias estimation using multi-GNSS observations and global ionosphere maps. Navigation: Journal of the Institute of Navigation, 61(3), 191-201. https://doi.org/10.1002/navi.64
21. Subirana, J. S., Zornoza, J.M., Hernández, M. (2013). GNSS Data Processing, Vol. I: Fundamentals and Algorithms. Pajares, Contactivity bv, Leiden, the Netherlands, ISBN 978-92-9221-886-7
22. Ignacio, R. (2021). RINEX. The Receiver Independent Exchange Format Version 4.00. IGS/RTCM RINEX WG, Darmstadt, Germany, 120.
23. Astafyeva, E. (2019). Ionospheric detection of natural hazards. Reviews of Geophysics, 57(4), 1265-1288. https://doi.org/10.1029/2019RG000668

24. Komjathy, A., Yang, Y. M., Meng, X., Verkhoglyadova, O., Mannucci, A. J., & Langley, R. B. (2016). Review and perspectives: Understanding natural-hazards-generated ionospheric perturbations using GPS measurements and coupled modeling. Radio Science, 51(7), 951-961. https://doi.org/10.1002/2015RS005910
25. Laštovička, J. (2022). Long-term changes in ionospheric climate in terms of foF2. Atmosphere, 13(1), 110. https://doi.org/10.3390/atmos13010110
26. Naumov, A. O., Khmarskiy, P. A., Byshnev, N. I., & Piatrouski, N. A. (2023). Methods and software for calculating total electronic content based on GNSS data. Advanced Engineering Days (AED), 7, 158-160.